Non-uniform Time Resampling for Diagnosing Broken Rotor Bars in Inverter-fed Induction Motors

Tomas Alberto Garcia-Calva, *Student Member, IEEE*, Daniel Morinigo-Sotelo, *Member, IEEE* and Rene de Jesus Romero Troncoso, S*enior Member, IEEE*

Abstract*—Fault detection in inverter-fed induction motors is an actual industrial need. Many line-fed machines are being replaced by inverter-fed drives for improving control during startup and also for saving energy. Broken rotor bars in induction motors is one of the most difficult faults to be detected, particularly when the motor is fed by an inverter in a soft startup. The difficulty of detecting broken rotor bars is that the characteristic fault-related frequencies are very close to the fundamental frequency, and the amplitude of the fundamental is significantly higher than the fault-related frequency components. This paper proposes an effective method that allows the detection of the broken rotor bar fault in inverter-fed induction motors during a soft startup transient based on a non-uniform resampling algorithm. The proposed algorithm transforms the non-stationary fundamental frequency into a stationary component by non-uniform resampling, whereas the fault-related components are considerably separated from the fundamental one, making easier to follow their evolution during the startup transient. Simulation and experimental results demonstrate the effectiveness of the proposed method to detect the fault.

***Index Terms*— condition monitoring, fault detection, induction motors, inverters, multiple signal classification, non-uniform sampling.**

Manuscript received February 28, 2016; revised April 18, 2016; accepted September 20, 2016. This work was supported in part by the Mexican Council of Science and Technology CONACYT scholarship 572940; Universidad Autonoma de Queretaro sabbatical scholarship 2015-2016; Universidad de Guanajuato DAIP grant No. 733/2016; Universidad de Valladolid grant for foreign professors in the doctoral program 2015-2016; and by the Spanish Ministerio de Economía y Competividad and FEDER program in the framework of the Proyectos I+D del Subprograma de Generación de Conocimiento, Programa Estatal de Fomento de la Investigación Científica y Técnica de Excelencia Ref: DPI2014-52842-P.

T. A. Garcia-Calva is with the DICIS, University of Guanajuato, Salamanca, 36885. Mexico (e-mail: ta.garciacalva@gmail.com).

D. Morinigo-Sotelo is with the Electrical Engineering, University of Valladolid, 47014. Spain (e-mail: daniel.morinigo@eii.uva.es).

R. J. Romero-Troncoso is with CA Telematica, DICIS Universidad de Guanajuato, Salamanca 36885, Mexico (corresponding author phone: +52-464-6479940; fax: +52-464-6479940; e-mail: troncoso@hspdigital.org).

I. INTRODUCTION

THE induction motors (IM) are the most important electric machines in many industrial applications due to their excellent performance, low cost and robustness [1]. Although these machines are reliable and very rugged, the possibility of unexpected faults is unavoidable [2-3]. From all faults that IM can develop, the presence of a broken rotor bar (BRB) is one of the most difficult to detect. This type of fault may not show any early symptoms, propagating to the next bars and leading to a sudden collapse, producing an abrupt interruption of the process. Previous research works have dealt with the monitoring and detection of this fault, even at early stages of development, [4-6], but there is still opportunity to make contributions to the field. It is well known that BRB induces multiple current harmonics in the stator windings. The technique for broken bar detection is performed by measuring the sideband current harmonics, named left-side (LSH) and right-side (RSH) harmonics [7-8]. They appear close to the fundamental frequency component of the power supply (FC), where the separation between them depends on the rotor slip *s*. However, these frequency components are significantly affected by the inverter operation where the main voltage frequency is not fixed, the slip is usually low and spurious harmonics are induced.

Some methods have been proposed to detect the BRB of inverter-fed IM. For instance, in [9-10], a high-frequency signal is injected in different spatial directions of the machine, and the impedance is calculated. Wolbank *et al.* [11] proposed monitoring a rotor bar defect using the inverter to establish a voltage pulse excitation and the built-in current sensors to extract the fault indicators. However, these methods require the motor to be disconnected from the load in order to make a measurement in standstill. Nonetheless, this option is not acceptable in many cases for economic and technical concerns. Therefore, a number of methods based on the steady-state current analysis of inverter-fed IM have been studied. For instance, [12-15] proposed the frequency analysis of stator current using different methods. Göktas *et al.* [16] presented a study using analytical signal angular fluctuation. In [17] an approach for condition monitoring using wavelets is proposed. Although several techniques have been utilized for a steady-state analysis, the BRB fault is tough to detect in an inverter fed system. The analysis based on the transient current presents potential advantages in comparison with the

analysis based on steady-state. The reason is that fault signatures in the time-frequency domain provide additional information than the information provided by the frequency spectrum only. In the frequency spectrum, the information consists in the amplitude that the spectral components have in specific frequency locations, without indicating the time when they appear. The information from the time-frequency analysis consists in the trajectories that the spectral frequency components follow along the time line, not just the location of the components in the frequency domain. The presence of these trajectories in the time-frequency domain indicates that the motor has a fault, [18]. Some techniques have been proposed to detect BRB under the aforementioned conditions. For instance, in [19] the fractional Fourier transform is used to facilitate the fault diagnosis. Cusido *et al.* [20] proposed the Short-Time Fourier Transform (STFT) in combination with a Wavelet analysis to detect BRB with good results. In [21] an adaptive transform uses a function called the time-frequency atom; this permits a precise observation of fault components in transient regimes, even if they are close to the main component. However, all the research works mentioned above require a previous knowledge of the time evolution of the fault harmonics. Different techniques have been proposed to overcome the aforementioned drawback. For instance, Stefani *et al.* [22] applied a demodulation technique by using a generator stator current in induction machines. In [23], it has been proposed a methodology based on a modified version of the Prony´s method that provides a high-frequency resolution and an adjustable time resolution. Nevertheless, there are not many works related to the detection of BRB in IM under the operating conditions produced by an inverter during the startup transient. It is still necessary to further explore other methodologies.

Discrete resampling methods are promising signal processing techniques recently used for fault detection of rotating machinery. Digital resampling converts transient signals into stationary ones, and this facilitates an effective diagnosis of mechanical faults in wind turbines [24-27]. On the other hand, it is proposed in [28] a resampling method for the extraction of spatial-domain information and to track the deterioration in electrified vehicle gearboxes. Zhu *et al.* [29] proposed a turbocharger quality inspection system, in which the resampling method is used to analyze vibrations generated by the turbocharger running at variable speed. These results demonstrate that the proposed techniques based on resampling work well on extracting non-stationary harmonics from the sampled data. Despite the efforts made in the cited papers, the implementation of these methods required a large memory, a shaft encoder or complex observers for implementation. Therefore, it is desired a method that could provide accurate BRB fault detection in IM under startup transient based on the resampling method and without additional hardware.

This paper proposes a novel method for detecting the presence of a BRB in inverter-fed IM during a startup transient at reduced voltage and low slip. The proposed approach consists in separating the fault-related harmonics from the- FC via a non-uniform time resampling, evading spectral overlap and smearing. The use of this technique permits the separation of the-BRB components from the FC and provides a very clear pattern in the spatial-frequency domain to detect the fault. In the proposed method, the voltage and current signals are uniformly sampled in the time domain. According to the frequency characteristics of the voltage signal, the non-uniform time resampling is then performed for the current signal such that the FC and its harmonics are converted to constant values. The multiple-signal classification (MUSIC) method is used as spectral estimation method of the spatial-frequency decomposition to identify the fault signature, which is a characteristic trajectory of the LSH in the spatial-frequency domain. The proposed method is validated by a theoretical study and experimental results for the detection of one BRB. In these experiments, the uniform sampling is compared to the non-uniform sampling; then, the MUSIC spectral estimation method is compared to the well-known Welch and Burg spectral estimation methods; afterwards, three different operating frequencies of the inverter feeding the motor are tested; finally, the effects on the fault detection of different mechanical loads are compared. The proposed technique has the advantage of not requiring any additional hardware for measuring or estimating the rotating speed. Moreover, the low computational cost of the proposed strategy permits its implementation in low-cost equipment such as digital signal processors (DSP) or field-programmable gate array (FPGA), which will allow us online fault detection.

II. BACKGROUND

This section introduces the basic theoretical framework used in this work.

A. Broken Rotor Bar Fault

The detection of broken rotor bars in IM can be done by observation of the sideband harmonics f_{BRB} components as:

$$f_{BRB} = f_{\sup}\left[k\left(\frac{1-s}{p}\right) \pm s\right] \tag{1}$$

where s is the per-unit motor slip, p is the number of pole pairs of the motor, $k/p = 1,3,5...$ are the characteristics values of the motor, and $f_{\sup}$ is the electrical supply frequency [8].

B. MUSIC Algorithm

The subspace methods are known as high-resolution methods that detect frequencies with low signal-to-noise ratio. The subspace methods assume that the discrete-time sequence $x[n]$ can be represented by *m* complex sinusoids in noise $e[n]$, [30]; i.e.

$$x[n] = \sum_{i=1}^{m} \overline{B}_i e^{j2\pi f_i n} + e[n], \quad n = 0,1,2,\cdots N-1 \tag{2}$$

with

$$\overline{B_i} = |B_i| e^{\phi_i} \tag{3}$$

where N is the sample length, $\overline{B_i}$ is the complex amplitude of the *i*-th complex sinusoid, f_i is its frequency $e[n]$ is a sequence

of white noise with zero mean and variance σ^2 .This method uses the eigenvector decomposition of $x[n]$ to obtain two orthogonal subspaces. The autocorrelation matrix $\mathbf{R}$ of the noisy $x[n]$ is the sum of signal and noise autocorrelation matrices ($\mathbf{R}_s$ and $\mathbf{R}_n$ respectively):

$$\mathbf{R} = \mathbf{R_s} + \mathbf{R_n} \sum_{i=1}^{P} |B_i|^2 \mathbf{e}(f_i)\mathbf{e}^H(f_i) + \sigma_n^2 \mathbf{I} \tag{4}$$

where p is the number of frequencies and the exponent H denotes Hermitian transpose, $\mathbf{I}$ is the identity matrix and $\mathbf{e}^H(f_i)$ is the signal vector given by:

$$\mathbf{e}^H(f_i) = [1 \;\; e^{-j2\pi f_i} \;\; \cdots \;\; e^{-j2\pi f_i(N-1)}] \tag{5}$$

From the orthogonality condition of both subspaces, the MUSIC pseudo-spectrum Q is given by:

$$Q^{MUSIC}(f) = \frac{1}{\left|\mathbf{e}^H(f)\mathbf{v}_{m+1}\right|^2} \tag{6}$$

where $\mathbf{v}_{m+1}$ is the noise eigen-vector. This expression exhibits the peaks that are exactly at frequencies of principal sinusoidal components where $\mathbf{e}^H(f)\mathbf{v}_{m+1} = 0$, [31].

In this work, a short-time MUSIC approach is computed to obtain a time-frequency signal representation. The short-time MUSIC is constructed by partitioning the signal into small segments by using a sliding window; then each segment is processed by the MUSIC algorithm, realizing a sliding-window pseudo-spectrum of the signal. The short-time MUSIC mitigates the effects of noise, evidencing only larger frequency components. detection.

III. Proposed Non-Uniform Time Resampling

In Inverter-Fed IM during the startup transient, the fundamental voltage frequency is not fixed and the slip becomes very low. Under the above conditions, the left-side component, whose magnitude must be monitored for diagnostic purposes, evolves in time parallel and very close to the fundamental component. It turns out that the direct application of motor current signature analysis (MCSA) to the stator current is not effective. A simple solution for an efficient diagnosis of BRB in inverter-fed IM during the startup transient is presented here via non-uniform time resampling.

A. Resampling

Resampling is an approach to determine the value of a discrete-time sequence at arbitrary points in time. It denotes the transformation of a discrete-time sequence with a given sampling frequency f_i into a discrete-time sequence having a different sampling frequency f_o .In the general resampling method, the sequence $x(n) = x(nT_i)$, sampled with the input sampling period T_i or correspondingly sampling frequency f_i, is transformed into the sequence $y(m) = y(mT_o)$, sampled with the output period T_o or correspondingly sampling frequency f_o. The ratio between the output and the input frequency is referred to as the conversion factor or the resampling ratio

$$R = \frac{f_o}{f_i} = \frac{T_i}{T_o} = \frac{L}{M} \tag{7}$$

where L and M are integers. The resampling process can be conceptually modeled as a resampling filter [32]. Let $h(k)$ be the impulse response of the prototype filter. The time domain relationship among $x(n)$, $h(k)$ and $y(m)$ is

$$y(m) = \sum_{k=-\infty}^{\infty} h(Mm - kL)x(k) \tag{8}$$

The spectrum of $y(m)$, can be determined in terms of the spectrum of $x(n)$ and the resampling ratio L/M as

$$Y(e^{j\omega}) = \frac{L}{M} X(e^{j\omega L/M}) \tag{9}$$

An expansion or compression occurs in the spectrum due to the resampling technique, proportional to the L/M ratio. If the time resampling ratio R is kept constant, the resampling method is said to be uniform; otherwise, if the time resampling ratio R varies according to a certain relationship, the resampling method is said to be non-uniform.

B. Non-Uniform Time Resampling

Non-uniform time resampling establishes a time-dependent relationship for the fundamental frequency in such a way that it becomes a function of time $R(t) = f(t)$. Then, the original uniform time sampled $x(n)$ is converted into the resampled signal $y(m)$ with a time-dependent resampling ratio $R(t)$.

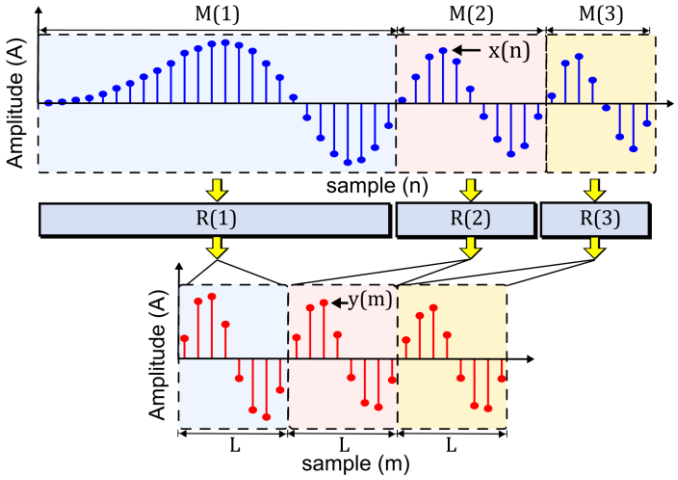

Fig. 1. Illustration of a non-uniform time resampling of a chirp signal.

For the proposed methodology, the resampling ratio is selected to be:

$$R(t) = \frac{L}{M(t)} \tag{10}$$

where L is set constant and $M(t)$ is selected to be the number of uniform samples that each cycle of the fundamental frequency contains and its value is adjusted for each cycle.

This way, if the *i*-th cycle of the original signal contains $M_i(t)$ uniform samples, the resampling rate is set to L/M_i and the resampled signal will have exactly L samples. Because L is fixed, each cycle of the resampled signal will contain the same number of samples, L, making the fundamental frequency of the resampled signal a stationary component. The proposed method computes the signal resampling with a non-uniform factor in time for each cycle of the original signal. Fig.1 illustrates how a non-uniform time resampled sinusoid chirp is resampled into a signal with the fundamental frequency made stationary. Three cycles of the original signal are shown, each with a different quantity of samples, and after the resampling process, the chirp signal becomes a sinusoid signal with constant frequency, having L samples in each resulting cycle.

The proposed algorithm is used to resample the stator current of an inverted-fed IM at the startup transient as illustrated in Fig.2.

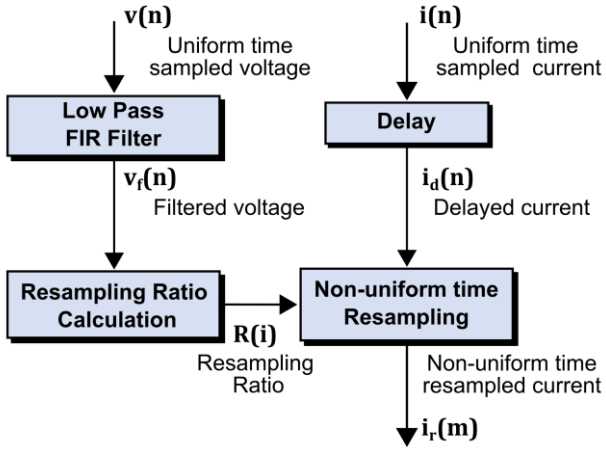

Fig. 2. Schematic of the non-uniform time resampling method applied to the stator current signal.

In the proposed method, one phase of the stator voltage and current are measured for BRB detection. The overall algorithm is described as follows:

1) Acquire the stator current and voltage signals with a fixed and uniform sampling frequency f_i. The result is $v(n)$ and $i(n)$ where $n = 1,2,3,\ldots,N$; being N the sample length of the stator voltage and current uniform acquisitions.
2) Filter the voltage signal from noise to obtain the fundamental component of the voltage supply; the resulted filtered signal is $v_f(n)$.
3) Delay the stator current signal by the same amount of the voltage filter group delay; the result is $i_d(n)$.
4) Obtain the number of samples per cycle $M(i)$, with $i = 1,2,3,..Nc$, from the filtered voltage signal $v_f(n)$ as reference by counting the samples between two zero-crossings during each *i*-th cycle.
5) Calculate the non-uniform resampling ratio $R(i) = L/M(i)$, where L is the target number of samples for each cycle of the voltage signal in order to convert it into a stationary signal with constant frequency $f = f_i/L$.
6) Resample the uniform current signal $i_d(n)$ at the non-uniform time resampling rate $R(i)$. The result sequence is the non-uniform time resampled stator current $i_r(m)$.

C. Theoretical Validation

To validate the proposed methodology, the major components of a stator phase voltage and stator phase current are synthetically generated:

$$v_s(t) = V_s \sin(\omega_f t) \tag{11}$$

$$i_s(t) = I_f \sin(\omega_f t + \alpha) + I_l \sin(\omega_l + \alpha_l) + I_r \sin(\omega_r + \alpha_r) \tag{12}$$

where $V_f, I_f, \alpha, \alpha_l, \alpha_r$, are the amplitude of the fundamental voltage component, the amplitude of the fundamental current component, phase angle of the fundamental component, phase angle of the left and right side BRB components, respectively.

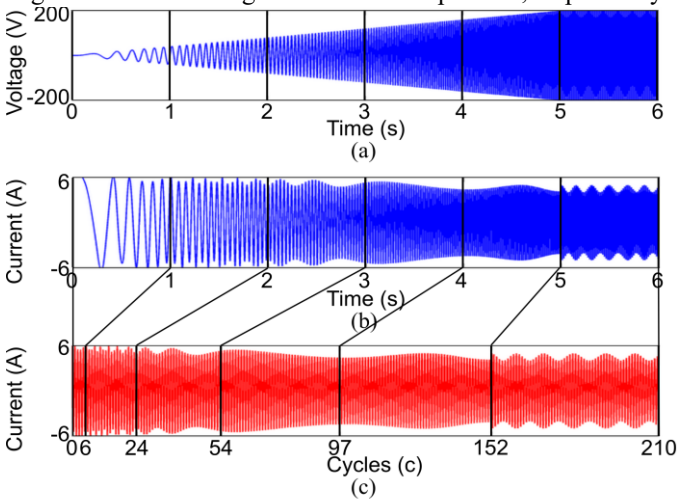

Fig. 3. Theoretical time domain startup transient of an IM with a BRB fault: (a) Uniformly-sampled voltage, (b) Uniformly-sampled current, (c) Non-uniformly resampled current.

The frequency pattern $\omega_{r,l} = (1 \pm s)\omega_s$ is produced in the IM current due to the BRB fault. The corresponding synthetic stator voltage and current are depicted in Fig. 3a and 3b, respectively. Fig. 3c shows the resampled stator current via the non-uniform time resampling. Notice that first second of the current signal is mapped into 6 cycles; the next second is mapped into 18 cycles, whereas the following seconds are mapped into 30, 43, 55 and 61, respectively. This is due to the non-uniform time intervals of the original signal for each cycle.

The theoretical time evolutions of the main frequency components contained within the stator current of an inverted-fed IM during 5s startup transient followed by 1s of a steady-state regime are shown in Fig. 4. The figure has been plotted assuming a linear variation in time of the f_c fixed by the

inverter, from 0 to 60Hz in 5s, and a rotor frequency from 0 to 57 Hz during the same time interval. BRB fault related harmonics are dependent of the motor slip, which is given by:

$$s = \frac{f_C - f_r}{f_C} \tag{13}$$

During the soft startup operation of the motor, gradually controlled by the inverter, the rotor speed changes very slowly and the BRB fault related frequencies evolve very close to the fundamental frequency [21]. Fig. 5 depicts the theoretical evolution of the FC, LSH, and RSH after the stator current is non-uniformly time resampled. The figure shows how the fundamental frequency is transformed into a stationary component, whereas the LSH and RSH fault-related components are separated from the fundamental one, facilitating the identification of their evolution trajectories. This separation of the LSH and RSH from the fundamental component, due to the proposed method of non-uniform resampling, improves the diagnosis of the BRB fault.

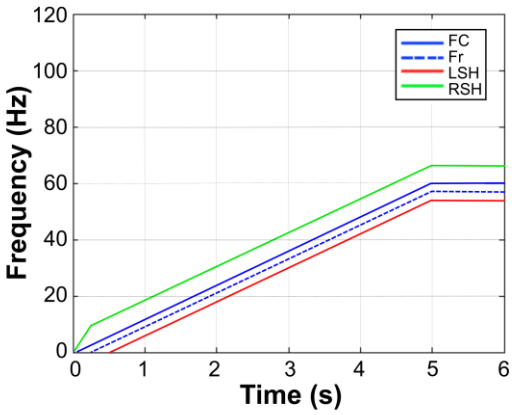

Fig. 4. Theoretical trajectories of the fundamental component (Fc), the rotor frequency (Fr) and the fault related harmonics, left-side (LSH) and right-side (RSH), of the uniformly sampled stator current signal.

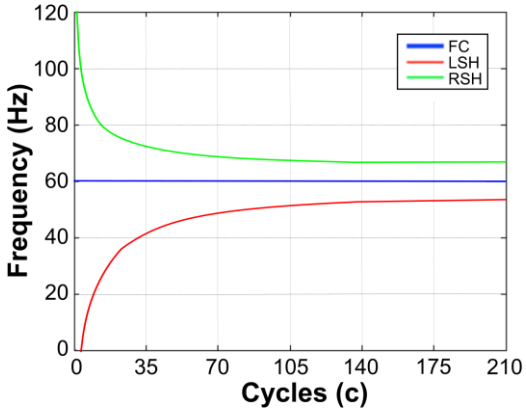

Fig. 5. Theoretical trajectories of the fundamental component (Fc), the left side harmonic (LSH) and the right side harmonic (RSH) of the non-uniform time resampled stator current.

IV. Experimental Setup

The experimental setup consists in using a soft startup controlled by an inverter model WEG CFW08 to feed the motor under test. The startup signal consists in a linear ramp from 0 to the nominal 220 V_{AC} with the frequency increasing from 0 to a selected operating frequency in a period of 5s. Fig. 6a shows the experiment setup where two different 1-hp three-phase induction motors (model WEG 00136APE48T) are used for testing the performance of the proposed methodology. The tested motors have 2 poles, 28 bars and a rated voltage supply of 220 V_{AC}. The applied mechanical load consists in an ordinary alternator. The current signal is acquired using a hall-effect sensor model L08P050D15, from Tamura Corporation. A 16-bit 4-channel serial-output sampling analog-to-digital converter ADS8341 from Texas Instrument Incorporated is used in a proprietary data acquisition system. The sampling frequency is set to f_i = 12 kHz obtaining 60,000 samples during 5s of the induction motor startup transient and 12,000 samples during 1s of the steady state regime. The BRB condition is produced by drilling a 2.0 mm diameter hole in a bar of the rotor, without harming the rotor shaft. Fig. 6(b) shows the rotor with the broken bar used during the test.

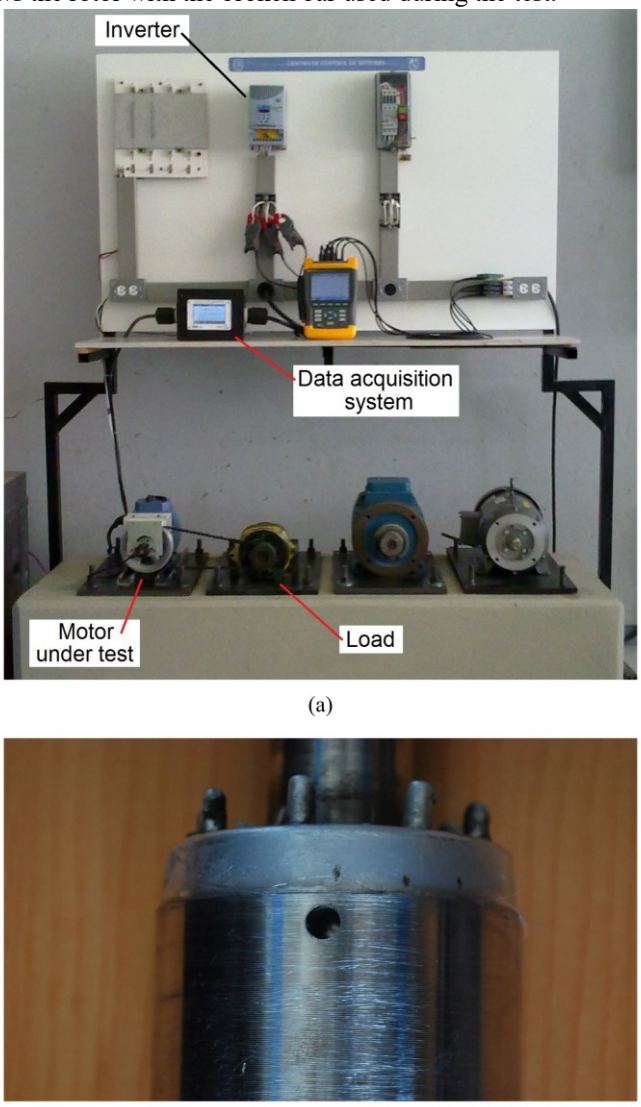

Fig. 6. (a) Experimental setup of the test bench. (b) Rotor with one broken rotor bar.

Four experimental cases of study are developed to test the proposed method under different conditions of interest for the fault diagnosis. All experimental cases of study compare the results between the healthy motor and the motor with the broken rotor bar condition. The first case of study makes the comparison between the uniform sampling and non-uniform resampling, whereas the rest of the conditions are fixed. The second case of study compares the efficiency of MUSIC as spectrum estimation method vs. the Welch and Burg methods. The third case of study presents the effects of different operating frequencies at the inverter that feeds the motor. And the fourth case of study shows the effects of changing the mechanical load at the motor.

V. Experimental results

In the four cases of study, and for all the conditions that are compared, each condition under comparison is presented in three graphs. The first graph presents the spatial-frequency decomposition of the healthy condition of the motor, the second graph shows the spatial-frequency decomposition of the motor with the broken rotor bar, and the third graph is obtained as the difference between the faulty to the healthy condition. The third graph is a detection indicator of the presence of the fault because it enhances the presence of the LSH component when it is present, while suppressing the fundamental frequency, which results in an enhanced plot of the presence of the fault.

The signal processing of the acquired experimental data is implemented in the Matlab Digital Signal Processing Toolbox. To reduce the computation time and to optimize the pseudo-spectrum estimation, after the data acquisition stage, the signal is decimated. As a result, the frequency region, where the fault frequency evolution of the broken rotor bar condition will be observed, is limited to the 0-120 Hz frequency range. In all studied cases, the stator voltage and current signals have the same time duration of 6s: 5s covering the soft startup transient and 1s for the steady-state regime. The stator current signal is divided into segments of 200 data points each one.

A. Case 1 Uniform vs. Non-uniform Resampling

In the first case of study the operating frequency is set to 60 Hz with a mechanical load representing half (50%) of the nominal load for the motor and MUSIC as spectrum estimation method. In this experiment it is compared the difference obtained between using a uniform sampling rate (standard method) and a non-uniform sampling rate (proposed method).

The MUSIC algorithm, with a modal order of 6, is used to analyze each segment of the spatial-frequency decomposition, and the result forms the sort-time ST-MUSIC pseudo-spectrum.

The results of this case of study are depicted in Fig. 7. Fig. 7(a) depicts the pseudo-spectrum of the uniformly sampled current signal of a healthy motor, whereas Fig. 7(b) shows the uniformly sampled current signal of the motor with one BRB. Fig. 7(c) depicts the detection indicator for the uniform sampling. Notice that the LSH is almost imperceptible for a uniform sampling. On the other hand, Fig. 7(d) depicts the non-uniform resampled current signal of the healthy motor; Fig. 7(e) shows the non-uniform resampled current signal of the motor with one BRB, and Fig. 7(f) depicts the detection indicator graph of the non-uniform resampling method. In these cases, it can be noticed that the fundamental frequency has been transformed into a stationary signal and the LSH is separated from the FC, making its trajectory in the spatial-frequency domain clearly visible in the corresponding pseudo-spectrum.

In the results of the healthy motor, it is remarkable that the fundamental frequency becomes a constant value in the spatial-frequency domain, and there are no other spectral components present. Regarding the results of the faulty motor, in Fig. 7(c), it is barely noticeable the presence of the LSH caused by a BRB fault. Meanwhile, Figs. 7(d) to 7(f) show the results of the non-uniform resampled stator current analysis for the healthy and faulty motors. The proposed method converts the fundamental component trajectory into a horizontal line. This transformation makes easier to distinguish the evolution of the fault-related component, even when the slip is low, because the LSH trajectory is separated from the trajectory of the main harmonic. Therefore, the detection of the faulty condition is improved when the non-uniform time resampling algorithm is applied to stator current.

Figs. 7(d) to 7(f) are used for comparison to the rest of the cases of study.

B. Case 2 Spatial-frequency decomposition

The second case of study uses a non-uniform sampling rate with 60 Hz of operating frequency and 50% of mechanical load. This experiment compares the efficiency of the spectrum estimation methods between Welch, Burg and MUSIC. Figs. 7 and 8 comprise the results of this comparison. Figs. 8(a) to 8(c) present the spatial-frequency decomposition for the Welch method of the healthy motor, the motor with the BRB, and the detection indicator graph, respectively. Figs. 8(d) to 8(f) depict the graphs for the Burg method and Figs. 7(d) to 7(f) show the graphs for the MUSIC method.

From this comparison it can be noticed that the MUSIC spatial-frequency decomposition method gives clearer results for detecting the presence of the LSH indicating the fault than the Welch and Burg methods. The performance of MUSIC is better than Welch and Burg methods in the presence of noise.

C. Case 3 Effects of the operating frequency

The third case of study uses a non-uniform sampling rate with MUSIC as spectrum estimation method and 50 % of mechanical load. This experiment compares the effects of three different operating frequencies set to 12, 30, and 60 Hz. Figs. 7 and 9 contain the results of this comparison. Figs. 9(a) to 9(c) present the spatial-frequency decomposition for the operating frequency set at 12 Hz; Figs. 9(d) to 9(f) depict the spatial-frequency decomposition for the operating frequency set at 30 Hz; and Figs. 7(d) to 7(f) show the spatial-frequency decomposition for the operating frequency set at 60 Hz.

Results show that the proposed method is able to detect the presence of the LSH component of the BRB fault for all the operating frequencies at the inverter from 12 and up to 60 Hz.

D. Case 4 Effects of different mechanical loads

The fourth case of study uses a non-uniform sampling rate with MUSIC as spectrum estimation method and 60 Hz of operating frequency. Three load conditions are compared with no load, 50%, and 100% of nominal load. Figs. 7 and 10 present the results of this comparison. Figs. 10(a) to 10(c) present the spatial-frequency decomposition for the motor driving no mechanical load; Figs. 7(d) to 7(f) depict the spatial-frequency decomposition for the motor driving 50% of the nominal mechanical load; and Figs. 10(d) to 10(f) show the spatial-frequency decomposition for the motor driving 100% of the nominal mechanical load.

In this case of study, the proposed method is able to detect the presence of the fault-related LSH component when the motor is mechanically loaded; yet, the presence of the fault is not noticeable when the motor is working with no load, which is a limitation of the method. Anyhow, a motor working with no load is not a realistic operating condition because the motor in general always drives a load, where the proposed method is effective in detecting the presence of the fault.

E. Computational cost

The proposed method is implemented under Matlab in a desktop PC with an Intel Core i7 CPU running at 3.1 GHz and 8-GB RAM. The complete method includes three computational stages: digital filtering, resampling process, and spatial-frequency decomposition. Once the signal is acquired, the digital filtering stage is computed in 1.30ms and the resampling process takes 33.20ms to be computed. The spatial-frequency decomposition lasts 93.70ms, 275.10ms, and 359.31ms for the Welch, Burg, and MUSIC methods, respectively. The total computation time is 128.20ms, 309.60ms, and 393.81ms whether the Welch, Burg or MUSIC spatial-frequency decomposition method is used. Considering that the acquisition process takes 6s and the proposed method takes below 0.5s, the computational burden is kept low.

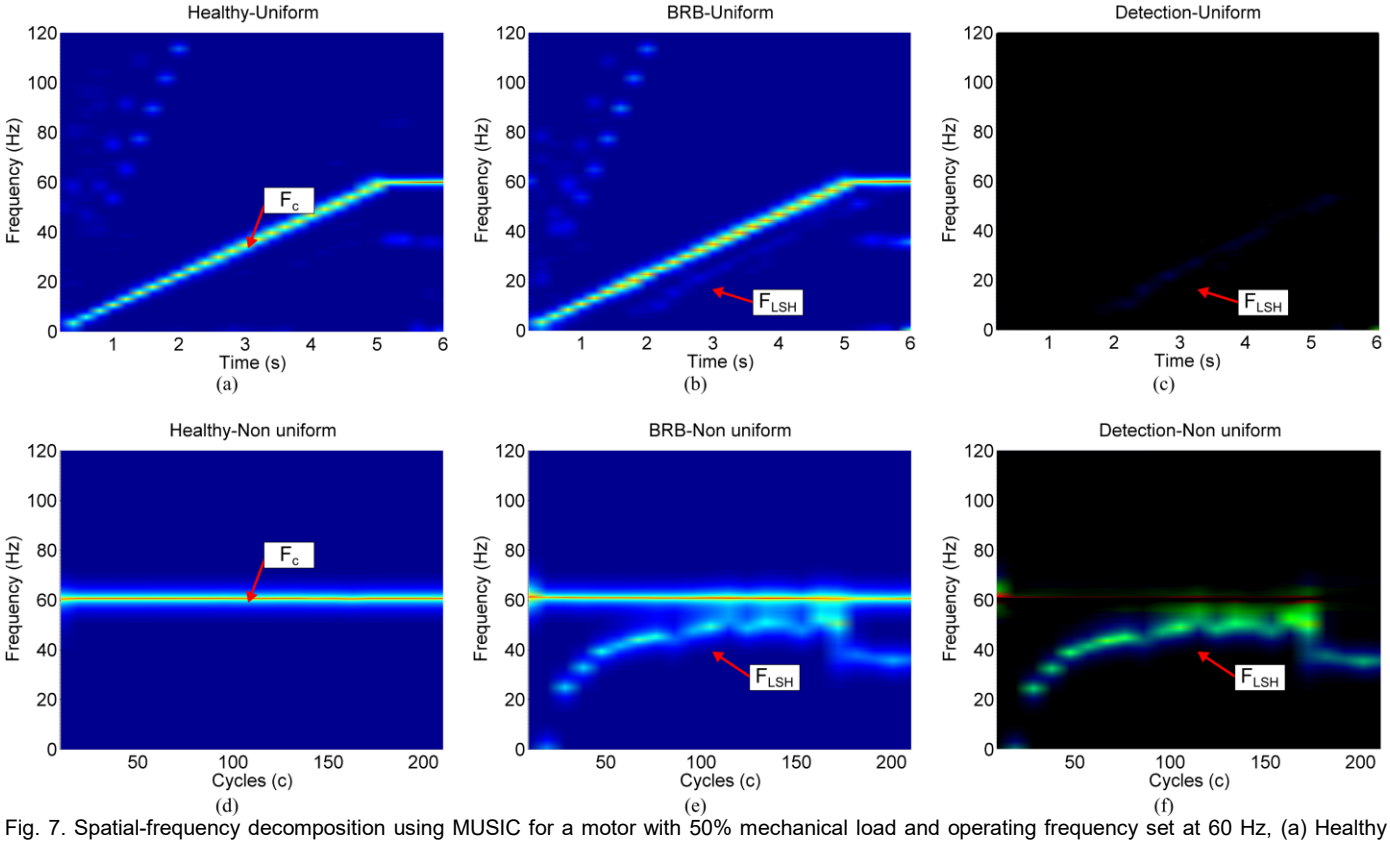

Fig. 7. Spatial-frequency decomposition using MUSIC for a motor with 50% mechanical load and operating frequency set at 60 Hz, (a) Healthy with uniform sampling, (b) BRB and uniform sampling, (c) Detection indicator with uniform sampling, (d) Healthy with non-uniform sampling, (e) BRB with non-uniform sampling, and (f) Detection indicator with non-uniform sampling.

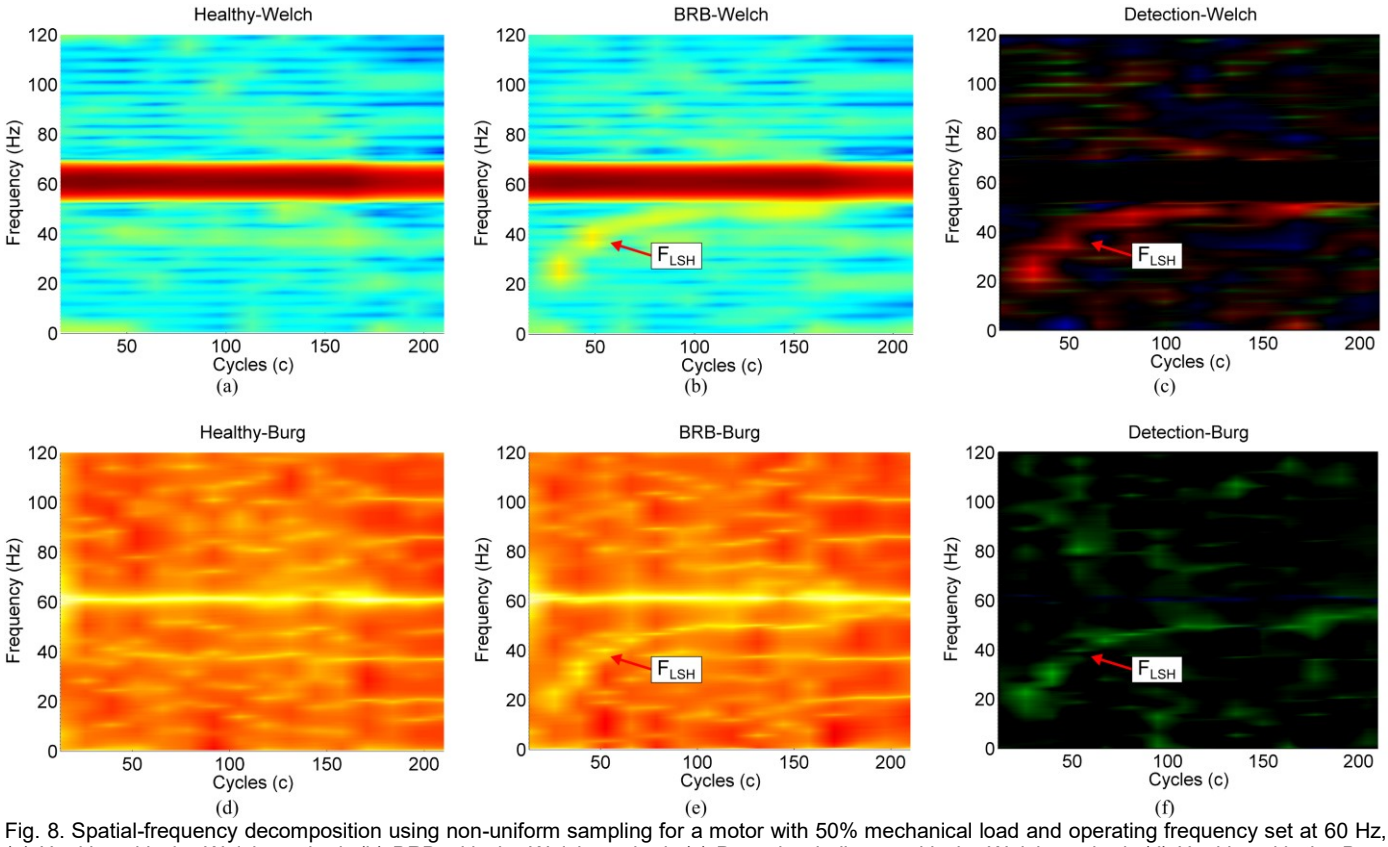

Fig. 8. Spatial-frequency decomposition using non-uniform sampling for a motor with 50% mechanical load and operating frequency set at 60 Hz, (a) Healthy with the Welch method, (b) BRB with the Welch method, (c) Detection indicator with the Welch method, (d) Healthy with the Burg method, (e) BRB with the Burg method, and (f) Detection indicator with the Burg method.

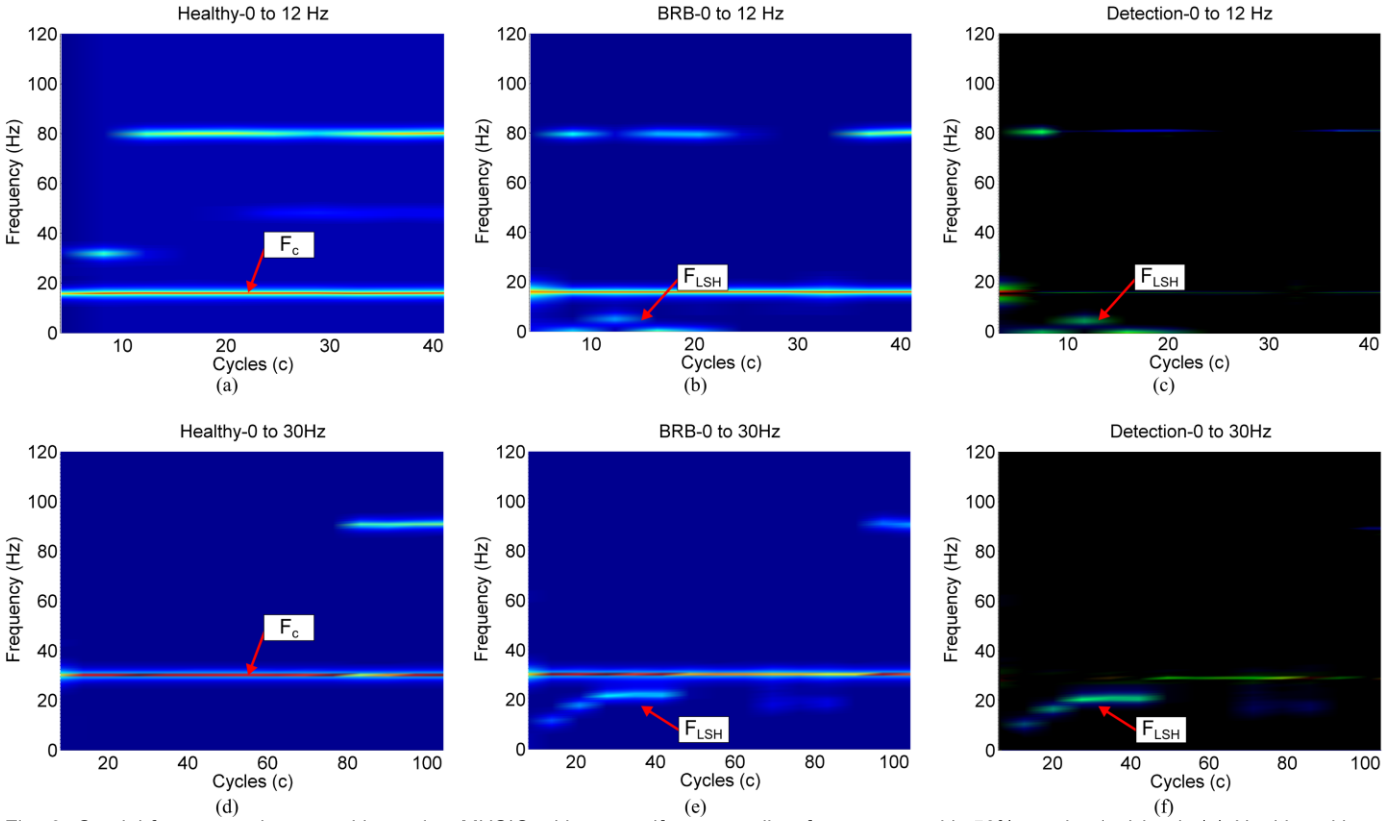

Fig. 9. Spatial-frequency decomposition using MUSIC with non-uniform sampling for a motor with 50% mechanical load, (a) Healthy with an operating frequency set at 12 Hz, (b) BRB with an operating frequency set at 12 Hz, (c) Detection indicator with an operating frequency set at 12 Hz, (d) Healthy with an operating frequency set at 30 Hz, (e) BRB with an operating frequency set at 30 Hz, and (f) Detection indicator with an operating frequency set at 30 Hz.

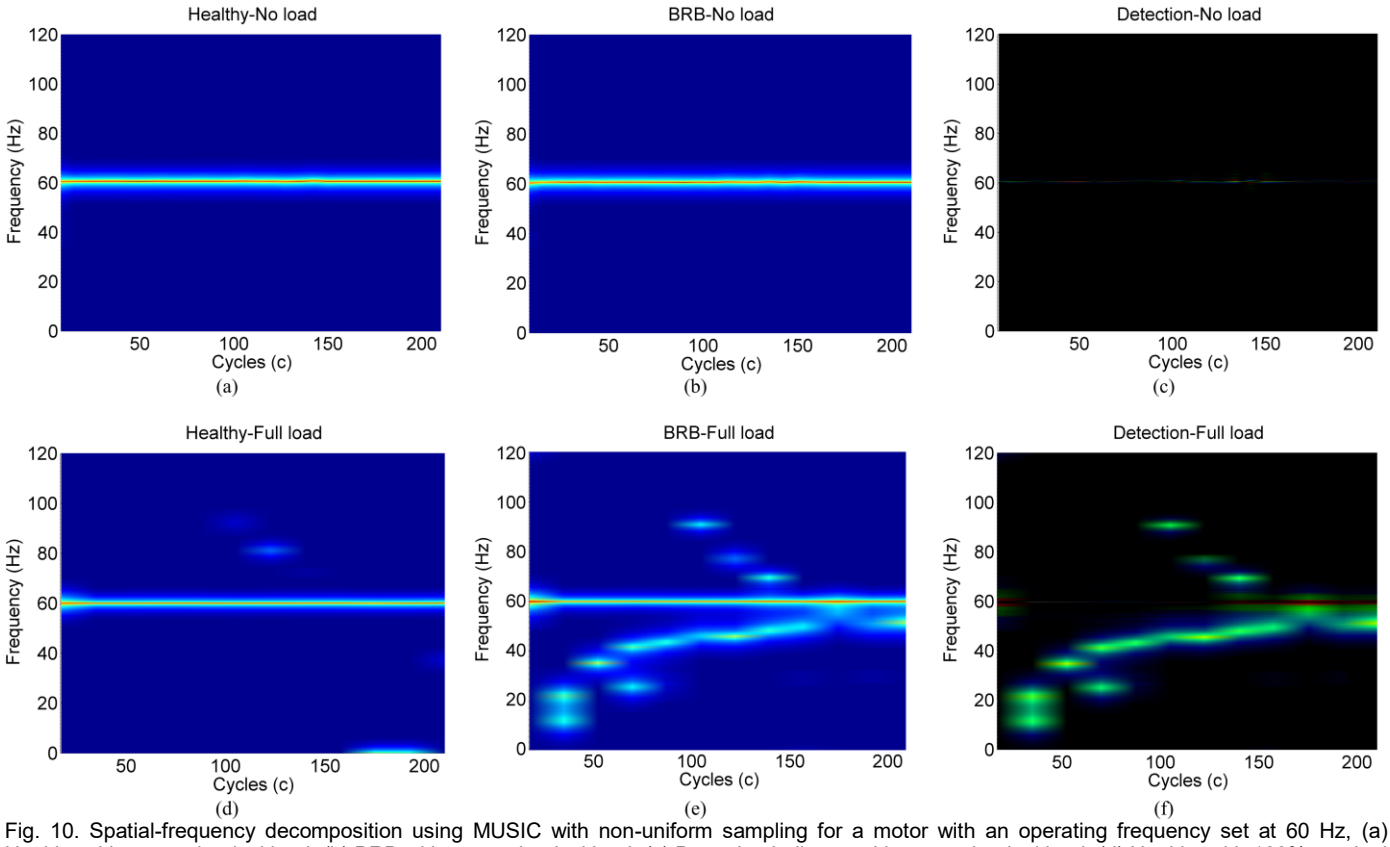

Fig. 10. Spatial-frequency decomposition using MUSIC with non-uniform sampling for a motor with an operating frequency set at 60 Hz, (a) Healthy with no mechanical load, (b) BRB with no mechanical load, (c) Detection indicator with no mechanical load, (d) Healthy with 100% nominal load, (e) BRB with 100% nominal load, and (f) Detection indicator with 100% nominal load.

VI. Conclusions

In this paper, a novel methodology for the diagnosis of broken rotor bars in inverter-fed induction motors is presented. The proposed method consists in a non-uniform resampling of the stator current signal with the voltage source from the inverter as the reference signal for the resampling process. The result is a separation of the fault-related harmonic trajectory from fundamental component evolution. This transformation of the trajectories facilitates the observation and identification of the progression of the fault-related components during a soft startup transient. Furthermore, the method overcomes the disadvantage of spectral leakage and can be used at a very low slip IM operation. Moreover, the proposed method does not require using speed sensors or speed estimation techniques. Experimental results have confirmed the effectiveness and advantages of the proposed methodology for the diagnosis of broken rotor bars in induction motors fed by inverters. The technique can also be applied to detect other faults in inverter-fed IM during soft startup transients.

References

[1] H.A. Toliyat, and G.B. Kliman, *Handbook of Electric Motors*, 2nd ed., USA: CRC Press. 2004, c, pp.35-41.

[2] W.T. Thomson and M. Fenger, “Current signature analysis to detect induction motor faults,” *IEEE Ind. Appl. Mag.*, vol. 7, no. 4, pp. 26–34, Jul./Aug. 2001.

[3] F. Filippetti, A. Bellini, and G.A. Capolino, “Condition monitoring and diagnosis of rotor faults in induction machines: State of art and future perspectives,” in *Proc. IEEE Workshop Rlrct. Mach. Desing, Control Diagnosis,* Paris, Mar. 2013, pp. 196-207.

[4] R. Romero-Troncoso, D. Morinigo-Sotelo, O. Duque-Perez, P. Gardel-Sotomayor, R. Osornio-Rios, and A. Garcia-Perez, “Early broken rotor bar detection techniques in VSD-fed induction motors at steady-state,” in *Proc. IEEE Int. Symp. Diagnostics Elect. Mach., Power Electron. Drives*, 2013, pp. 105–113.

[5] T.M. Wolbank, and G. Stojicic, "Monitoring of partially broken rotor bars in induction machine drives," in *Proc. Annu. Conf. IEEE Ind. Electron. Soc*., 2010, pp. 912-917.

[6] J.J. Rangel-Magdaleno, R.J. Romero-Troncoso, R.A. Osornio-Rios, E. Cabal-Yepez and L.M. Contreras-Medina, "Novel methodology for online half-broken-bar detection on induction motors," *IEEE Trans. Instrum. Meas.*, vol. 58, no. 5, pp. 1690-1698, May 2009.

[7] M. Pineda-Sánchez, M. Riera-Guasp, J.A. Antonino-Daviu, J. Roger-Folch, J. Pérez-Cruz, and R. Puche-Panadero, “Instantaneous frequency of the left sideband harmonic during the startup transient: a new method for diagnosis of broken bars,” *IEEE Trans. Ind. Electron*., vol. 56, no. 11, pp. 4557–4570, Nov. 2009.

[8] M.E.H. Benbouzid, “A review of induction motors signature analysis as a medium for faults detection,” *IEEE Trans. Ind. Electron.,* vol. 47, no. 5, pp. 984–993, Oct. 2000.

[9] B. Kim, K. Lee, J. Yang, S.B. Lee, E.J. Wiedenbrug, and M.R. Shah, "Automated detection of rotor faults for inverter-fed induction machines under standstill conditions," *IEEE Trans. Ind. Appl*., vol. 47, no. 1, pp. 55-64, Jan.-Feb. 2011.

[10] S.B. Lee, J. Yang, J. Hong, J.Y. Yoo, B. Kim, K. Lee, J. Yun, M. Kim, K.W. Lee, E. Wiedenbrug, and S. Nandi, "A new strategy for condition monitoring of adjustable speed induction machine drive systems," *IEEE Trans. Power Electron.,* vol.26, no.2, pp. 389-398, Feb.2011.

[11] T.M. Wolbank, P. Nussbaumer, H. Chen, and P.E. Macheiner, "Monitoring of rotor-bar defects in inverter-fed induction machines at zero load and speed," *IEEE Trans. Ind. Electron.,* vol.58, no. 5, pp.1468-1478, May 2011.

[12] L.A. Garcia-Escudero, O. Duque-Perez, D. Morinigo-Sotelo, and M. Perez-Alonso, "Robust multivariate control charts for early detection of broken rotor bars in an induction motors fed by a voltage source inverter," in *Proc. 2011 IEEE Power Eng., Energy Elect. Drives Int. Conf.* pp.1-6.

[13] H. Razik, M.B. Correa, and E.R.C. Silva, "A novel monitoring of load level and broken bar fault severity applied to squirrel-cage induction motors using a genetic algorithm," *IEEE Trans. Ind. Electron.,* vol.56, no.11, pp.4615-4626, Nov. 2009.

[14] O. Duque-Perez, L.A. Garcia-Escudero, D. Morinigo-Sotelo, P.E. Gardel, and M. Perez-Alonso, "Condition monitoring of induction motors fed by voltage source inverters. Statistical analysis of spectral data," in *Proc. Int. Conf. Elect. Mach.*, Sep. 2012, pp. 2479-2484.

[15] I.P. Georgakopoulos, E.D. Mitronikas, and A.N. Safacas, "Detection of induction motor faults in inverter drives using inverter input current analysis," *IEEE Trans. Ind. Electron.*, vol.58, no.9, pp.4365-4373, Sept. 2011.

[16] T. Göktas and M. Arkan, "Diagnosis of broken rotor fault in inverter-fed IM by using analytical signal angular fluctuation," in *Proc. Int. Power Electron. Motion Control Conf. Expo.*, 2014, pp.337-342.

[17] I.P. Georgakopoulos, E.D. Mitronikas, and A.N. Safacas, "Condition monitoring of an inverter-driven induction motor using Wavelets," in *Proc. Electromotion*, 2009, pp.1-5.

[18] J. Pons-Llinares, V. Climente-Alarcon, F. Vedreno-Santos, J.A. Antonino-Daviu, and M. Riera-Guasp, "Electric machines diagnosis techniques via transient current analysis," in *Proc. Annu. Conf. IEEE Ind. Electron. Soc.*, 2012, pp.3893-3900.

[19] M. Pineda-Sanchez, M. Riera-Guasp, J.A. Antonino-Daviu, J. Roger-Folch, J. Perez-Cruz, and R. Puche-Panadero, "Diagnosis of induction motor faults in the fractional Fourier domain," *IEEE Trans. Instrum. Meas.*, vol.59, no.8, pp.2065-2075, Aug. 2010.

[20] J, Cusido, L. Romeral, J.A. Ortega, J.A. Rosero, and A. Garcia-Espinosa, "Fault detection in induction machines using power spectral density in wavelet decomposition," *IEEE Trans. Ind. Electron.*, vol.55, no.2, pp.633-643, Feb. 2008.

[21] J. Pons-Llinares, D. Morinigo-Sotelo, O. Duque-Perez, J.A. Antonino-Daviu, and M. Perez-Alonso, "Transient detection of close components through the chirplet transform: Rotor faults in inverter-fed induction motors," in *Proc. Annu. Conf. IEEE Ind. Electron. Soc.,* 2014, pp.3386-3392.

[22] A. Stefani, A. Bellini, F. Filippetti, "Diagnosis of induction machines' rotor faults in time-varying conditions," *IEEE Trans. Ind. Electron.,* vol. 56, no. 11, pp.4548-4556, Nov. 2009.

[23] M. Sahraoui, A.J.M. Cardoso, K. Yahia, and A. Ghoggal, "The use of the modified Prony's method for rotor speed estimation in squirrel cage induction motors," *IEEE* Trans. Ind. Appl. vol. 52, no. 3, pp. 2194-2202, May-June 2016.

[24] X. Gong and W. Qiao, "Imbalance fault detection of direct-drive wind turbines using generator current signals," *IEEE Trans. Energy Convers.*, vol.27, no.2, pp.468-476, Jun. 2012.

[25] X. Gong and W. Qiao, "Current-based mechanical fault detection for direct-drive wind turbines via synchronous sampling and impulse detection," *IEEE Trans. Ind. Electron.*, vol.62, no.3, pp.1693-1702, Mar. 2015.

[26] L.F. Villa, A. Reñones, J.R. Perán, L.J. Miguel, "Angular resampling for vibration analysis in wind turbines under non-linear speed fluctuation" *Mech. Syst. Signal Process.,* vol. 25, no. 6, pp.2157-2168. Aug. 2011.

[27] H. Li, Y. Zhang and H. Zheng, "Angle domain average and CWT for fault detection of gear crack," in *Proc. Int. Conf. Fuzzy Syst. Knowledge Discovery,* vol.3, 2008, pp.137-141.

[28] C.M. Wolf, K.M. Hanson, R.D. Lorenz, and M.A. Valenzuela, "Using the traction drive as the sensor to evaluate and track deterioration in electrified vehicle gearboxes," *IEEE Trans. Ind. Appl.*, vol.49, no.6, pp.2610-2618, Nov.-Dec. 2013.

[29] D. Zhu and L. Lu, "Resampling method of computed order tracking based on time-frequency scaling property of Fourier transform," in *Proc. Int. Conf. Estimation Detection Inform. Fusion,* 2015, pp.248-253.

[30] S.H. Kia, H. Henao, and G.A. Capolino, "A high-resolution frequency estimation method for three-phase induction machine fault detection," *IEEE Trans. Ind. Electron.*, vol.54, no.4, pp.2305-2314, Aug. 2007.

[31] R.J. Romero-Troncoso, D. Morinigo-Sotelo, O. Duque-Perez, R. A. Osornio-Rios, M.A. Ibarra-Manzano, and A. Garcia-Perez, "Broken rotor bar detection in VSD-fed induction motors at startup by high-resolution spectral analysis," in *Proc. Int. Conf. Elect. Mach.,* Sep. 2014, pp.1848-1854.

[32] R.E. Crochiere *Multirate Digital Signal Processing* 1st ed. NJ, USA: Prentice-Hall, 1983, ch2, pp.29-47.

Tomas Alberto Garcia-Calva (S'07) received the B.S. degree in electronics engineering from the University of Guanajuato, Salamanca, Mexico, in 2014, where he is currently working toward the M.S. degree in electrical engineering. He was an Intern with the Universitat Politecnica de Valencia (UPV), Valencia, Spain in 2016. His research interests include hardware signal processing, multirate systems and diagnostics of electrical machines.

Daniel Morinigo-Sotelo (M'04) received the B.S. and Ph.D. degrees in electrical engineering from the University of Valladolid (UVA), Spain, in 1999 and 2006, respectively. He was a Research Collaborator on Electromagnetic Processing of Materials with the Light Alloys Division of CIDAUT Foundation since 2000 until 2015. He is currently with the Research Group in Predictive Maintenance and Testing of Electrical Machines, Department of Electrical Engineering, UVA and with the HSPdigital Research Group, México. His current research interests include condition monitoring of induction machines, optimal electromagnetic design, and heuristic optimization.

Rene de Jesus Romero-Troncoso (M'07–SM'12) received the Ph.D. degree in mechatronics from the Autonomous University of Queretaro, Queretaro, Mexico, in 2004. He is a National Researcher level 3 with the Mexican Council of Science and Technology, CONACYT. He is currently a Head Professor with the University of Guanajuato and an Invited Researcher with the Autonomous University of Queretaro, Mexico. He has been an advisor for more than 200 theses, an author of two books on digital systems (in Spanish), and a coauthor of more than 130 technical papers published in international journals and conferences. His fields of interest include hardware signal processing and mechatronics. Dr. Romero–Troncoso was a recipient of the 2004 Asociación Mexicana de Directivos de la Investigación Aplicada y el Desarrollo Tecnológico Nacional Award on Innovation for his work in applied mechatronics, and the 2005 IEEE ReConFig Award for his work in digital systems. He is part of the editorial board of Hindawi's International Journal of Manufacturing Engineering.